Calibrated Color Mapping Between LCD and CRT Displays: A Case Study

Behnam Bastani, Bill Cressman, Brian Funt
Simon Fraser University
Burnaby BC, Canada V5A 1S6

Abstract

The primary goal of a color characterization model is to establish a mapping from digital input values d_i (i=R,G,B) to tristimulus values such as XYZ. A good characterization model should be fast, use a small amount of data, and allow for *backward* mapping from tristimulus to d_i. The characterization models considered here are for the case of and end user who has no direct knowledge of the internal properties of the display device or its device driver. Three characterization models tested on seven different display devices are presented.

The characterization models implemented in this study are a 3D Look Up Table (LUT)[2], a linear model[5], and the masking model Tamura et al. in 2002[9]. The devices include two CRT Monitors, three LCD Monitors, and two LCD Projectors. The results of this study indicate that a simple linear model is the most effective and efficient for all devices used in the study. A simple extension to the linear model is presented, and it is demonstrated that this extension improves white prediction without causing significant errors for other colors.

Keywords

Color calibration, colorimetry, gamut mapping, color prediction

Introduction

Accurate color management across multiple displays is an important problem. Users are increasingly relying on digital displays for creating, viewing and presenting color imagery. Users with multi-panel displays would like to see color consistency across the displays, while conference speakers would like a more accurate prediction of what their slides will look like before they enter the auditorium. Of course, displays will have been characterized and calibrated by the manufacturer; nonetheless the end user may well wish to verify and improve upon the calibration. We present a study of techniques for end-user calibration of CRT and LCD displays.

Predicting colors across multiple display devices requires implementation of several concepts such as device characterization, gamut mapping, and perceptual models. The focus of this paper is device characterization by an end user, with the goal of selecting an appropriate model for mapping digital input values d_i (i=R,G,B) to tristimulus values such as XYZ, as well as *backward* mapping from XYZ to d_i. For example, if a user is interested in previewing an image on a one display as it will appear on a second display then a forward mapping is performed on the second display to predict XYZ values, and backward mapping is performed on the first display to select the best RGB coordinates for the best preview.

There are a several well-known characterization models that support both forward and backward mapping, three of which were implemented in this experiment: a 3D Lookup Table (LUT), a linear model and a masking model. The LUT method[2] uses a 3-dimensional table to associate a tristimulus triplet with every RGB combination and vice versa. This method is simple to understand but difficult and cumbersome to implement.

The term linear model refers to the group of models (GOG[3], S-Curve[9], and Polynomial[4] model) that estimate tristimulus response as a linear combination of primary color outputs. These models each start by linearizing the digital input response curves with a specific nonlinear function from which they draw their names. The linear model has been widely used for CRT monitors but has been criticized for its assumption of channel independence[9]**.** We will show a simple extension to the linear model (Linear+) that guarantees correct mapping of an important color (e.g., white) without adding significant errors to other colors.

The third model implemented in this study is the masking model introduced by Tamura, Tsumura and Miyake in 2002[9]. This model applies the concept of Under Color Removal (UCR) to mask inputs from 3-dimensional RGB space to 7-dimensional RGBCMYK space. It then linearizes the inputs and combines them with a technique similar to that used by the linear model.

This paper will discuss the implementation, benefits and pitfalls of each method with respect to use on CRT and LCD display devices. In general, prediction errors will be quantified terms of ΔE, as measured in 1994 CIE La*b* color space. The first section of the paper deals with data collection. The next section reviews the characteristics of the devices used in the study. Section Three discusses implementation details and considerations for each of the characterization models. Section Four reviews the results of the study.

Data Collection

All data used in this study was collected using a Photo Research SpectraScan 650 Spectroradiometer in a dark room with the spectroradiometer at a fixed distance, perpendicular to the center of the display surface. Before beginning each test, the monitor settings were re-set to the factory default, and the brightness was adjusted using a gray-scale calibration pattern until all shades of gray were visible.

The data collection was performed automatically in large, randomized test suites. We found that it is important to test the repeatability of the spectroradiometer with respect to each monitor, and ensure that the test plan is sufficient to smooth out the measurement errors. As a result, each RGB sample used in this study was derived from of a total of 25 measurements taken in 5 randomly scheduled bursts of 5 measurements each. This technique served to average out both long- and short-term variation. The size and quantity of bursts were determined through empirical study.

One issue that arises when using an automated data collection system is phosphor stabilization time. Figure XI shows the percentage of steady-state luminance for white (R=G=B=100) versus the number of seconds since a color change from black. “Luminance” as used here refers to the L value in $CIELAB_{94}$ space. Note that the LCD-based devices reach steady state within less than 5 seconds, while the CRT devices take longer—up to 10 seconds. The spike on CRT2 that occurs right after the color change is unexpected as well. In practice, we found that using a delay of 2500 ms between the display of a color and the start of measurement gave acceptable results.

An additional important setting related to data consistency is spectroradiometer integration time, which defines the number of milliseconds the spectroradiometer’s shutter remains open during a measurement. The integration time needs to be adjusted as a function of the incoming signal. In general, CRT monitors require a longer integration time because the display flashes with each beam scan. Figure XII shows the result of an integration time test on CRT1. Observe that shorter integration times result in more unstable measurements. The monitor refresh rate used in this experiment is 75 Hz, or 13.3 ms per scan. Therefore, any integration time t will experience either $\lfloor t/13.3 \rfloor$ or $\lceil t/13.3 \rceil$ scans depending on when the measurement window starts. For example, if the integration time is 100ms, then measurements will either experience seven or eight scans, leading to high variation. Conversely, a time of 400 ms will almost always lead to 30 scans (400 / 13.33 = 30.00).

The measurements in this study were taken with a default integration time of 400ms, which was doubled whenever a "low light" error was reported by the spectroradiometer and halved when a "too much light" error was reported. Although this technique resulted in acceptable error levels, an improvement would be to ensure that all integration times are exact multiples of 13.3, so each measurement gets the same number of scans.

Three suites of data were collected for each monitor: a 10x10x10 grid of evenly spaced RGB values covering the entire 3D space, a similar 8x8x8 grid used for testing and verification, and a "101x7" data set made up of 101 evenly spaced measurements for each RGB and CMYK channel with the other inputs set to zero.

Device characteristics

Seven devices were tested: two CRT monitors, three LCD monitors, and two LCD projectors. A summary of these devices is given in Table I. One important issue in characterizing a display is to determine the amount of channel interaction. In this study, channel interaction is calculated as follows.

$$CI_{RED}(v,a,b) = \frac{\big(L(v,a,b) - L(0,a,b)\big) - \big(L(v,0,0) - L(0,0,0)\big)}{L(255,255,255) - L(0,0,0)} \qquad (1)$$

In this equation, *v* represents the input value for the channel in question, *a* and *b* are constant values for the other two channels, and *L(r,g,b)* represents the measured luminance for a given digital input. The equations for CI_{GREEN} and CI_{BLUE} are similar. This equation measures how much the luminance of a primary changes when the other two channels are on. The overall interaction error for each device (Table I) was calculated as

$$Interaction = \frac{1}{N}\sum_{v=0}^{255} \left|CI_{RED}(v,255,255)\right| + \left|CI_{GREEN}(v,255,255)\right| + \left|CI_{BLUE}(v,255,255)\right| \qquad (2)$$

where N is the averaging factor = (255+1)*3.

From end-user point of view, three of the five LCD devices showed almost no channel interaction; however, both CRT monitors exhibited significant channel interaction (Figure XIII). The interaction on the CRT monitors was generally subtractive (leading to lower luminance) while on the LCD monitors it was either additive or negligible.

Another potential issue with LCD monitors is chromaticity shift of the primary colors. Figure XIV shows the chromaticity coordinates (after black correction) for each of the primary colors (RGB), as well as the secondary colors (CMY) and a tertiary color (K) plotted at 10 intensity settings per color. It was observed that all devices have stable RGB chromaticity; however, the LCD devices exhibited significant chromaticity shifts in the secondary colors, The cause of chromaticity shift is explained in detail by Marcu[11].

The presence of a chromaticity shift in the secondary colors (CMYK) causes problems with the masking model which uses the combined colors (CMYK) as additional primaries. The problem becomes apparent in the response-curve linearization step, where it is not be possible to find a single function that linearizes all three curves. As a result, the linearization is inexact which leads to erroneous output estimates.

Implementation Details

All characterization methods start with black-level correction in which the measured XYZ value of black (minimum output) for the device is subtracted from the measured tristimulus value of each color. This ensures that all devices have a common black point of (0,0,0) in XYZ space. Fairchild et. al. discuss the importance of this step[5]. The remaining steps for each characterization differ based on the method and are described below.

3D LUT Model

The 3D LUT method was implemented with the intention of providing a standard against which to evaluate the other two models[2]. It is expensive both in time and space (~10 MB for the lookup table) and is not well suited for reverse mapping. To create the forward lookup table, the 10x10x10 training data is interpolated using 3D linear interpolation to fill a 52x52x52 lookup table indexed by RGB values spaced 5 units apart. At look-up time, 3D spline interpolation is used to look up intermediate values.

Inverting the lookup to index by XYZ requires interpolation of a sparse 3D data set, which is non-trivial and an independent area of research[1]. The reverse lookup was performed via tetrahedral interpolation into the original 10x10x10 data set. Tetrahedral interpolation was chosen over a number of other methods primarily for its speed and its ability to handle sparse, irregularly spaced data.

Linear Model

The linear model is a two-stage characterization process. In the first step, the raw inputs d_i (i=1, 2, 3 for R, G, B) are linearized using a function $C_i(d_i)$ fitted for each channel. Linear regression is then used to

determine the slope M_{ij} between each linearized input $C_i(d_i)$ and the respective XYZ output where j=(1, 2, 3) for (X, Y, Z). The second stage applies matrix M to calculate estimated XYZ values.

$$\begin{bmatrix} X_{est} \\ Y_{est} \\ Z_{est} \end{bmatrix} = M \begin{bmatrix} C_1(d_1) \\ C_2(d_2) \\ C_3(d_3) \end{bmatrix} \quad (3)$$

The linearization function $C_i(d_i)$ is a 256-entry LUT calculated as follows. The measured response values for the i^{th} input channel are interpolated to obtain three output vectors $X(d_i)$, $Y(d_i)$ and $Z(d_i)$ in 256-dimensional space. Principal component analysis is then used to find the single vector $C_i(d_i)$ that best approximates all three vectors. The following equation calculates $C_i(d_i)$ where PCA_i represents the weighting vector obtained from principal component analysis for channel i.

$$C_i(d_i) = \begin{bmatrix} X(d_i) & Y(d_i) & Z(d_i) \end{bmatrix} * \begin{bmatrix} PCA_i \end{bmatrix} \quad (4)$$

In order to allow for backward mapping, two conditions are required: the linearization function must be monotonic and the matrix M must be invertible. Inversion of M is always possible because the input channels are linearly independent. However, the monotonicity requirement is a real problem with LCD displays where the response curves sometimes level out or even decline for high input values (Figure XV). It is therefore necessary to modify the linearization function to ensure monotonicity as shown in Figure XVI. Note that this modification, although necessary for backward mapping, reduces the accuracy of the linearization and increases the error of the forward characterization.

When creating the lookup table, a decision must be made regarding the size of the training data set. Figure XVII shows the effect of training size on the forward mapping error measured in ΔE. In general, a larger training set is better, but the benefit tapers off after about 10 data points. For the results section of this paper, a training data set with 101 points was used to ensure minimal error introduced by training data size.

The primary criticism of the linear model is that it assumes channel independence. As we have seen above, this is not always a valid assumption – even for CRT monitors. When there is channel interaction, the predicted XYZ output value for secondary and tertiary colors may not be accurate.

Predicting white and gray values correctly is crucial in color calibration[6]. White is generally the most significant on computer-generated images such as presentation slides or charts where there are large regions of pure white with no ambient lighting expected. We observed that the linear model in general overestimates the

luminance of white. There are several approaches to addressing this issue. One technique, WPPPLS, imposes a constraint so that the linear model emphasizes correct prediction of white[6].

A simple alternative approach is to apply a diagonal transform to the slope matrix *M* based on the measured and predicted values of pure white. The following formula shows the conversion, where $X_{MEASURED}$ is the measured X value for white and $X_{PREDICTED}$ is the predicted X value for white using the original slope matrix.

$$M_{LINEAR+} = M * \begin{bmatrix} \frac{X_{MEASURED}}{X_{PREDICTED}} & 0 & 0 \\ 0 & \frac{Y_{MEASURED}}{Y_{PREDICTED}} & 0 \\ 0 & 0 & \frac{Z_{MEASURED}}{Z_{PREDICTED}} \end{bmatrix} \quad (5)$$

This modification to the slope matrix ensures that white is correct, but slightly shifts all of the other colors in a non-uniform manner, which could potentially increase the overall error. This model will be referred to as "Linear+" in this paper, and is useful when displaying computer-generated images such as charts where white is a major color. Note that a similar correction can be performed using predicted values in an alternate space, such as LMS cone sensitivity space. In our study, we found that using either XYZ or LMS intermediate space returns the nearly same average increase in forward error (±0.05 ΔE for all devices) .

Further improvement may be possible using a technique similar to that presented by Finlayson and Drew in [6], where a modified least-squares procedure is used to determine the matrix *M*. By constraining the prediction error for white to zero, a matrix can be selected that reduces overall error while ensuring an accurate white value. It is interesting to note that their approach achieved good results even without first linearizing the inputs.

Masking Model

The masking model[9] attempts to avoid problems related to channel interaction with a technique similar to under color removal in printing. The original digital input d_i (i=1,2,3 for RGB) is converted to masked values m_i (i=1,2,3,4,5,6,7 for RGBCMYK), and the masked values are combined in a manner similar to that for the linear model. The masking operation assigns values to three elements of *m* – the primary color (index *p*), the

secondary color (index *s*), and the gray color (index 7), and sets all of the remaining elements of m to zero, as follows.

$$\begin{aligned}
\text{Primary color index } p \text{ such that } d_p &= \max(d_1, d_2, d_3) \\
\text{Under color index } k \text{ such that } d_k &= \min(d_1, d_2, d_3) \,\&\, k \neq p \\
\text{Secondary color index s} &= k + 3 \\
\text{Primary color} \quad m_p &= d_p \\
\text{Secondary color} \quad m_s &= d_{6-p-k} \\
\text{Gray (Under) color} \quad m_7 &= d_k \\
\text{Unused Color} \quad m_{q \notin \{p,s,7\}} &= 0
\end{aligned} \tag{6}$$

The result of these formulas is to set *p* to the index of the maximum primary color (R, G, or B), and m_p to the input value for that color. It assigns *s* to the index of the mixed color (C, M, or Y) that does not contain the minimum color, and assigns m_s to the median of the original values. Finally, it sets the gray (under color) value m_7 to the minimum of the three original inputs. For example, if the original inputs are RGB=(200,100,50), the primary color will be red, with a value of 200. The secondary color will be yellow (which does not contain blue) with a value of 100, and the gray (under) color will have a value of 50. The masked input array becomes *m*=[200,0,0,100,0,0,50].

Once the inputs have been converted into masked values m_i, a linearization function $C_i(m_i)$ for each input channel *i* is determined using the method described above for the linear model. The slope matrix M_{ij} for each input channel *i* and output channel *j* is calculated as using PCA and linear regression, also as described for the linear model. Finally, let the vector P_i represent the column of matrix *M* that contains the X, Y, and Z slopes for input channel *i*. The transformation from masked input to XYZ output can then be written as follows:

$$XYZ_{est} = \begin{bmatrix} P_p & P_s & P_7 \end{bmatrix} * \begin{bmatrix} C_p(m_p) - C_p(m_s) \\ C_s(m_s) - C_7(m_7) \\ C_7(m_7) \end{bmatrix} \tag{7}$$

The inverse mapping from XYZ to RGB is less obvious, and requires knowledge of the primary and secondary color indices *p* and *s*. There is no way to know these values, so all six possible (*p*, *s*) combinations are tested (RM, RY, GC, GY, BC, BM) and any combination that satisfies the following conditions will yield the correct result.

$$255 \;^{3}\; mp \;^{3}\; ms \;^{3}\; m7 \;^{3}\; 0 \qquad (8)$$

Results

We calculated values of forward error ΔE_{FWD}, round trip error ΔE_{TRIP}, and backward error ΔE_{BWD} for 512 colors in an 8x8x8 evenly spaced grid of RGB inputs. For each color, we found three vertices in CIE L*a*b* space: the measured value for the color v_M, the predicted value v_P, and a round-trip value $v_{RT.}$ The round-trip value was found by mapping backward and forward again from v_P. These points form a triangle with edges representing the forward, round-trip and backward error vectors. ΔE_{FWD} is the distance from v_M to v_P, ΔE_{TRIP} is the distance from v_P to v_{RT}, and ΔE_{BWD} is the distance from v_{RT} back to v_M.

With respect to forward or backward error, we see that the 3D LUT is the most accurate, followed by the linear, Linear+ and Masking models (Table II, Table III). Note, however, that the linear and masking models all have a round-trip error of zero, while the 3D LUT has a non-zero round-trip error indicating an imperfect inversion. This is not surprising considering the rounding error inherent in the sparse 3D interpolation required to build the backward lookup table.

A comparison of backward error distributions (Figure XVIII) shows that the linear model had the most compact distribution for each device, while the distribution for 3D LUT tended to have a number of high-error outliers. The cause of these outliers becomes apparent when the error values are plotted by chromaticity (Figure XIX). Observe that the largest errors for the 3D LUT are often on or near the gamut boundary.

For the linear model, the highest errors are fairly well distributed across the chromaticity space for all devices except the projectors, which have a distinct problem in the blue region. This is most likely due to the non-monotonicity exhibited by the projectors in the blue output curves (Figure XV). As mentioned in the implementation section, the monotonicity correction stage is a potential source of error for all devices. However, it appears to be adding very little error for devices that do not have a monotonicity problem (Table V). The most notable increase in error was seen with the Projector 1, which also had the most trouble with non-monotonicity.

The average error for the Linear+ model was nearly the same as that for the standard linear model. Recall that the goal of Linear+ is to guarantee that the predicted white is correct, at the possible expense of other colors predictions. The results in Table II and Table III show little increase in overall error, which means a

"perfect" white can be achieved without much degradation in other colors. Informal visual comparisons indicate that this model is often the best one to use for computer-generated graphics.

The masking model was expected to out-perform the linear model whenever there was an issue with channel interaction. However, the model's best performance (on CRT2) is only slightly better than that of the linear model. The primary pitfall of this model is that it depends on constant-chromaticity "combined primaries" (CMYK). It is clear from Figure XIV that this assumption fails for the LCD monitors and projectors used in this study. The chromaticity shift causes the input the linearization step to fail. Figure XX shows an example of an unsuccessful linearization for the black channel for PR1 in the masking model.

This explains why the performance of the masking model was better for the CRT monitors than any of the other devices– the CRTs do not have the shifting chromaticity problem. It is also interesting to note that on CRT2, the Linear+ algorithm introduced the largest amount of error, indicating that the interaction present on this monitor is not well suited for correction with non-uniform scaling.

With respect to efficiency, the linear model is the best. The linear model is slightly faster than the masking model and nearly 20 times faster than the 3D LUT. The linear model also requires less than half the storage space of the masking model, and less than $1/300^{th}$ the storage space required for 3D LUT (Table IV).

Conclusion

Several display characterization models were implemented in this paper: a 3D LUT, a linear model, an extension to the linear model, and a masking model. These characterization models were each tested on seven devices: two CRT Monitors, three LCD monitors and two LCD projectors. The devices are characterized from and end user perspective in which the devices are treated as black boxes with no knowledge or control over their internal workings.

In characterizing the devices, two issues that were of particular importance were phosphor stabilization time and spectroradiometer integration time (Figure XI, Figure XII). We found that the phosphor stabilization time on the CRT monitors can take up to 10 seconds. In practice, a delay time of 2500 ms between color display and measurement resulted in acceptable error levels. With respect to integration time, we propose that measurements on CRT monitors be taken with integration times that are multiples of the display scan rate. In addition, we observed that a training set of 10 data points per axis was sufficient for an accurate linear model for each of our 7 displays. (Figure XVII).

Although recent papers have indicated that the linear model is not applicable to LCD panels[9], it worked well for the LCD display tested in this experiment. Furthermore, the channel interaction problem was more pronounced on the CRT monitors than on several of the LCD displays. The fact that we did not find channel interaction with the LCD's we tested does not mean that it is not present in LCD panels themselves. We tested LCD displays which include electronics specifically designed to mitigate the effects of channel interaction. As a result, from an end-user point of view, channel interaction did not pose a problem. The primary issue with the LCD displays was the fact that the response curves for the three input channels were dissimilar, leading to chromaticity shift of combined colors (CMYK). This problem affected the masking model but not the linear model.

Despite these issues of linearization and channel interaction, all three models yielded a level of error that on average has a mean of less than 4 • E and a worst case less than 15 • E. The 3D LUT model was slightly more accurate than the other models, but it is too cumbersome for actual use. The linear model was the most efficient, with accuracy nearly as good as to the 3D LUT. A slight modification to the linear model is presented in the Linear+ model that uses a simple white-point correction technique to ensure correct prediction of white. Our results indicate the Linear+ model is able to guarantee white-point accuracy with minimal degradation for other colors.

Acknowledgements

The authors would like to thank Hewlett Packard Company, Creo Incorporated and the British Columbia Advanced Systems Institute for their financial contributions to this project.

Figure Captions

Figure I Percentage of the steady state luminance for white on the vertical axis versus the number of seconds since black was displayed on the horizontal axis.

Figure II: Measurement Error (Log scale) versus integration time in milliseconds measured for four grays on CRT1

Figure III: Channel Interaction. The horizontal axis represents the input value v ranging from 0 to 255 and the vertical axis represents the value of the channel interaction metric, $CI_{COLOR}(v,a,b)$. The black line shows a=b=255 and dashed lines show a=0,b=255 and a=255,b=0

Figure IV: Chromaticity shift shown as intensity is increased plotted in xy space with x=X/(X+Y+Z) on the horizontal axis and y=Y/(X+Y+Z) on the vertical axis. When there is no chromaticity shift, all the dots of one color lie on top of one another and therefore appear as a single dot. Color locations are indicated in the upper left panel by labels G, Y, R, C, K, M, B for green, yellow, red, cyan, black-to-white, magenta and blue respectively.

Figure V: Luminance curves for red, green, and blue phosphor input (Horizontal axis: R, G or B value. Vertical axis: L from Lab94)

Figure VI: Smoothing correction for non-monotonicity in the Z-response curve of the B channel for PR1

Figure VII: Mapping Error versus Training Data Size

Figure VIII: Backward Error distribution for each characterization model on each device. D*E error value is shown on the horizontal axis and histogram counts are shown on the vertical axis.*

Figure IX: Comparison of Outliers for the Backward model. Vertical axis and horizontal axes represent Y./(X+Y+Z) and X./(X+Y+Z) respectively. The • E error is plotted according to the legend of gray scales. The circular points represent outliers with • E greater than 1.5 times the average error. The majority of the high outlier errors for the LUT model occur near the gamut boundaries. . The outliers for linear model are quite negligible compared to the other two models.

Figure X: Linearization failure for the black channel on PR1

Figures

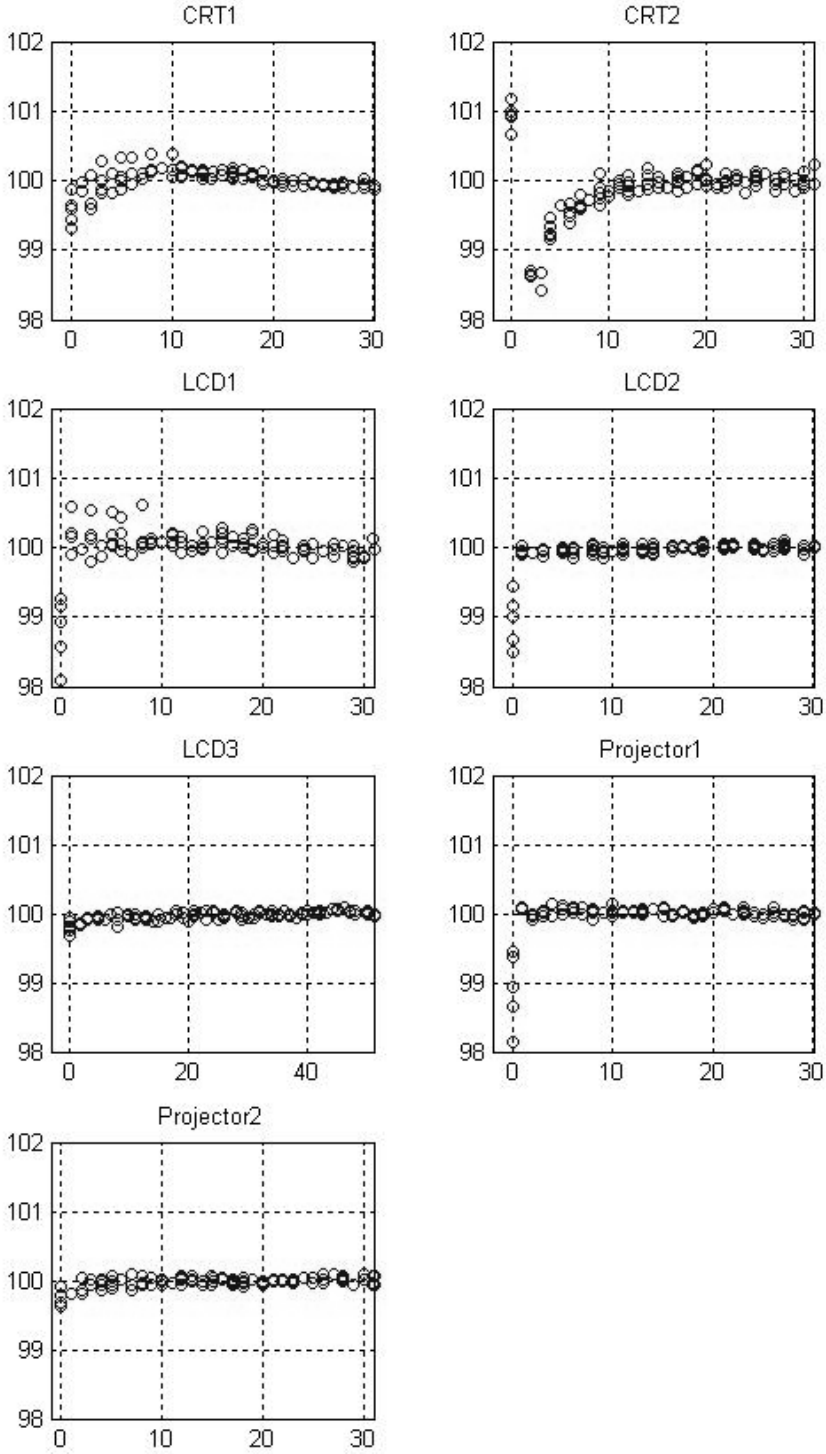

Figure XI Percentage of the steady state luminance for white on the vertical axis versus the number of seconds since black was displayed on the horizontal axis.

.

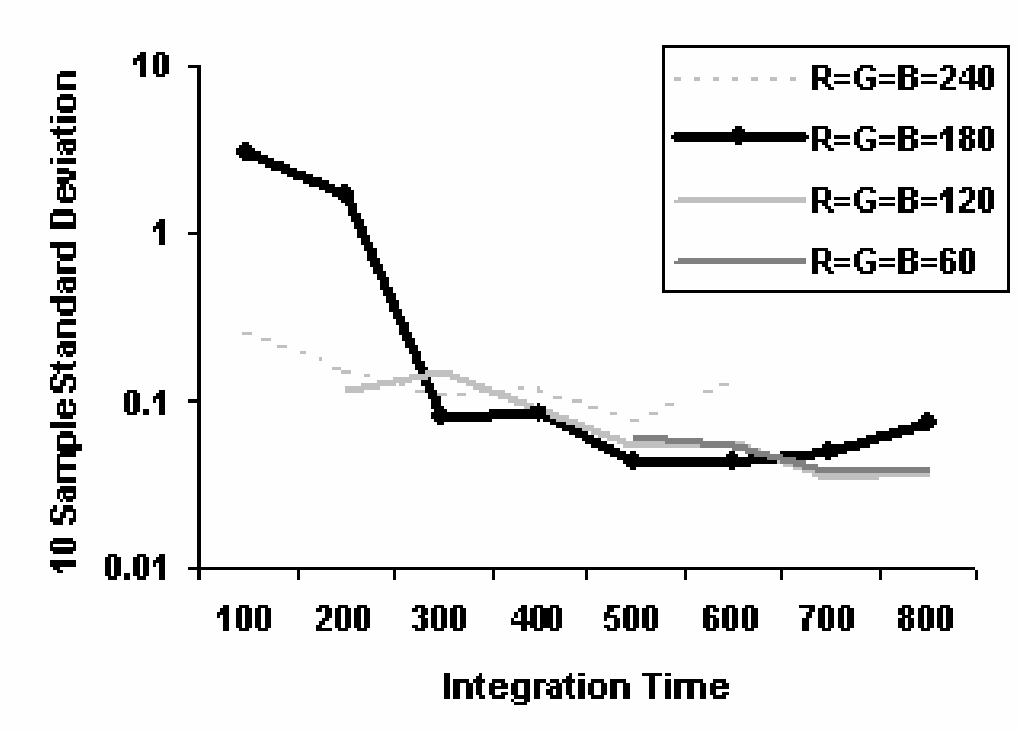

Figure XII: Measurement Error (Log scale) versus integration time in milliseconds measured for four grays on CRT1

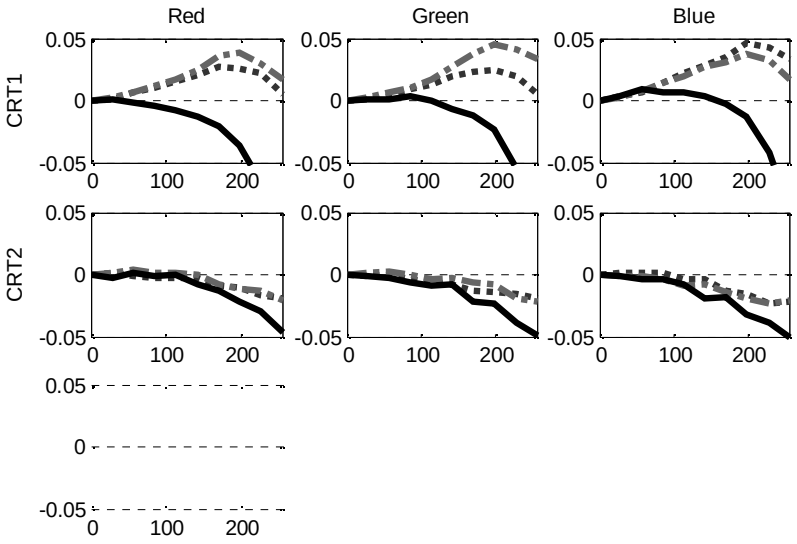
Red
Green
Blue
CRT1
CRT2
0.05
0
-0.05
0
100
200

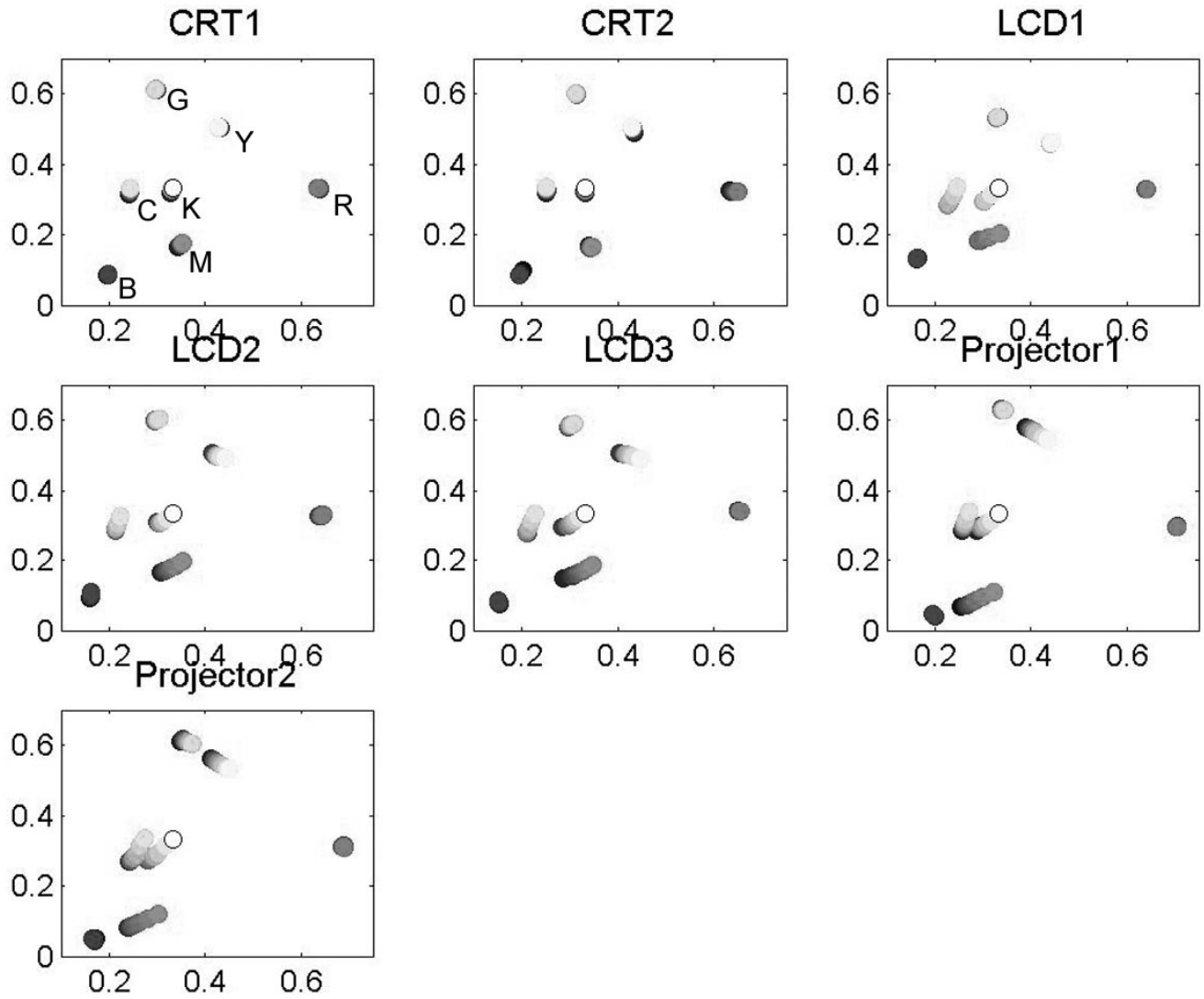

Figure XIV: Chromaticity shift shown as intensity is increased plotted in xy space with x=X/(X+Y+Z) on the horizontal axis and y=Y/(X+Y+Z) on the vertical axis. When there is no chromaticity shift, all the dots of one color lie on top of one another and therefore appear as a single dot. Color locations are indicated in the upper left panel by labels G, Y, R, C, K, M, B for green, yellow, red, cyan, black-to-white, magenta and blue respectively.

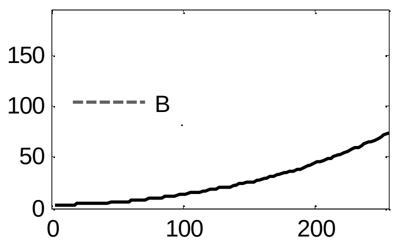

150
100
50
0
0
100
200
B

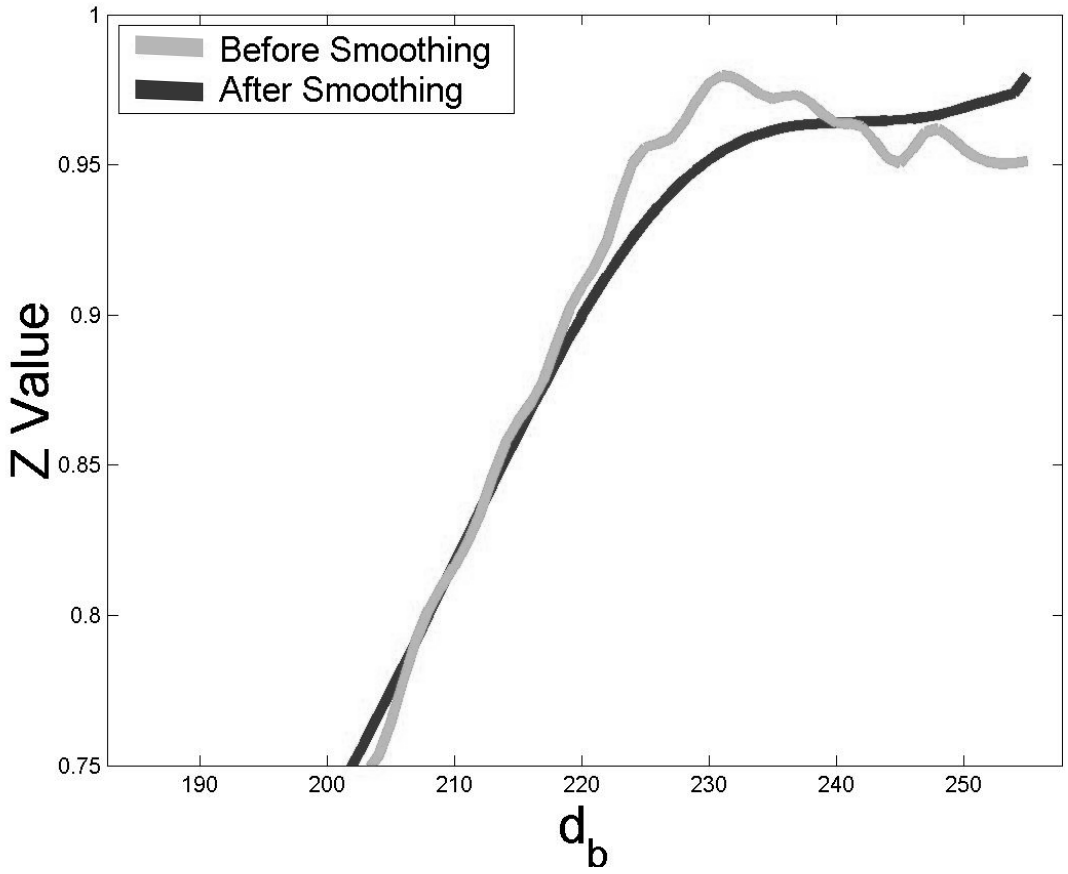

Figure XVI: Smoothing correction for non-monotonicity in the Z-response curve of the B channel for PR1

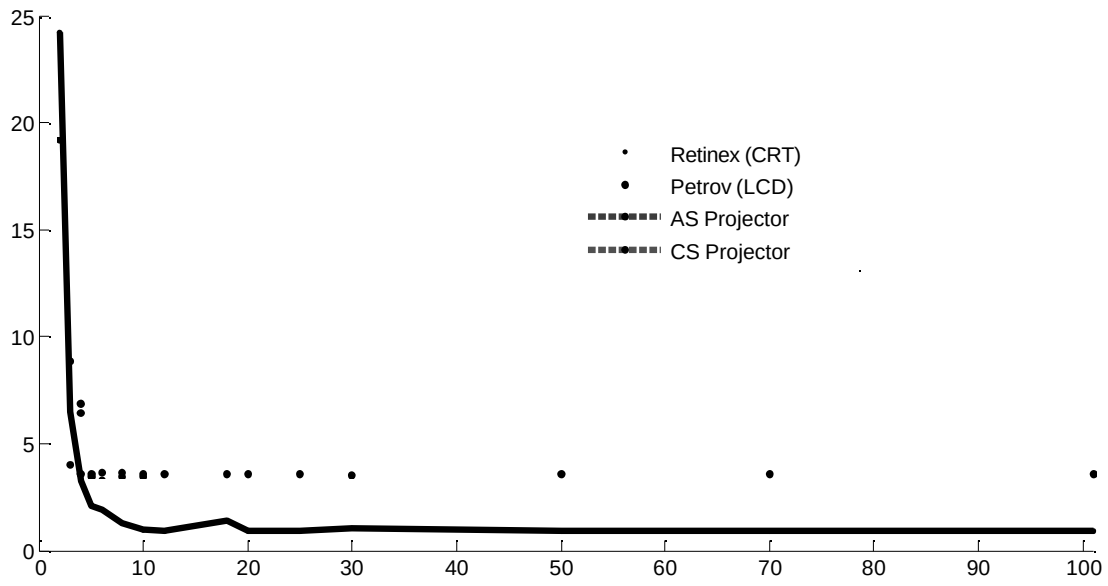
25
20
15
10
5
0
0
10
20
30
40
50
60
70
80
90
100
Retinex (CRT)
Petrov (LCD)
AS Projector
CS Projector

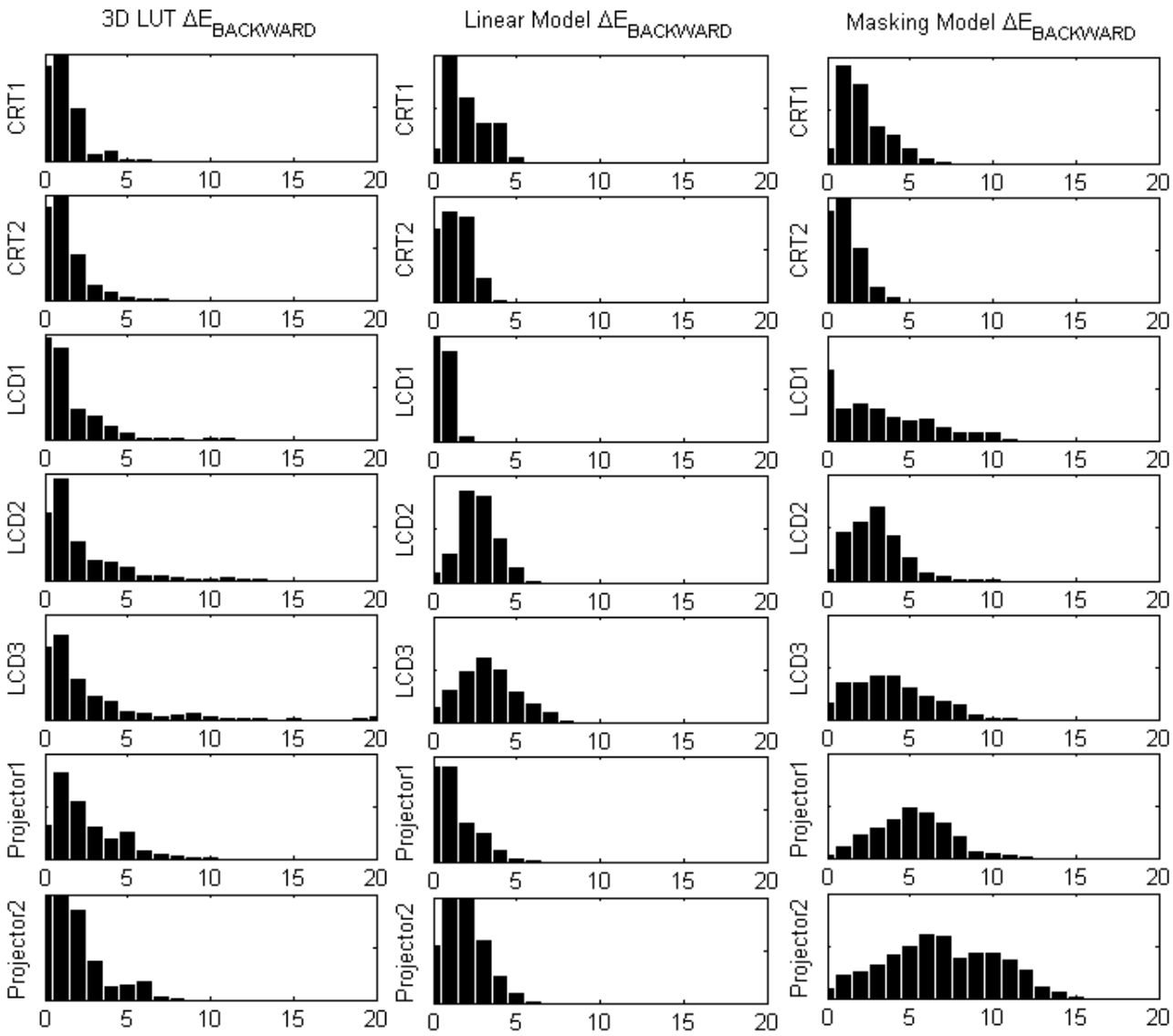

Figure XVIII: Backward Error distribution for each characterization model on each device. D*E error value is shown on the horizontal axis and histogram counts are shown on the vertical axis.*

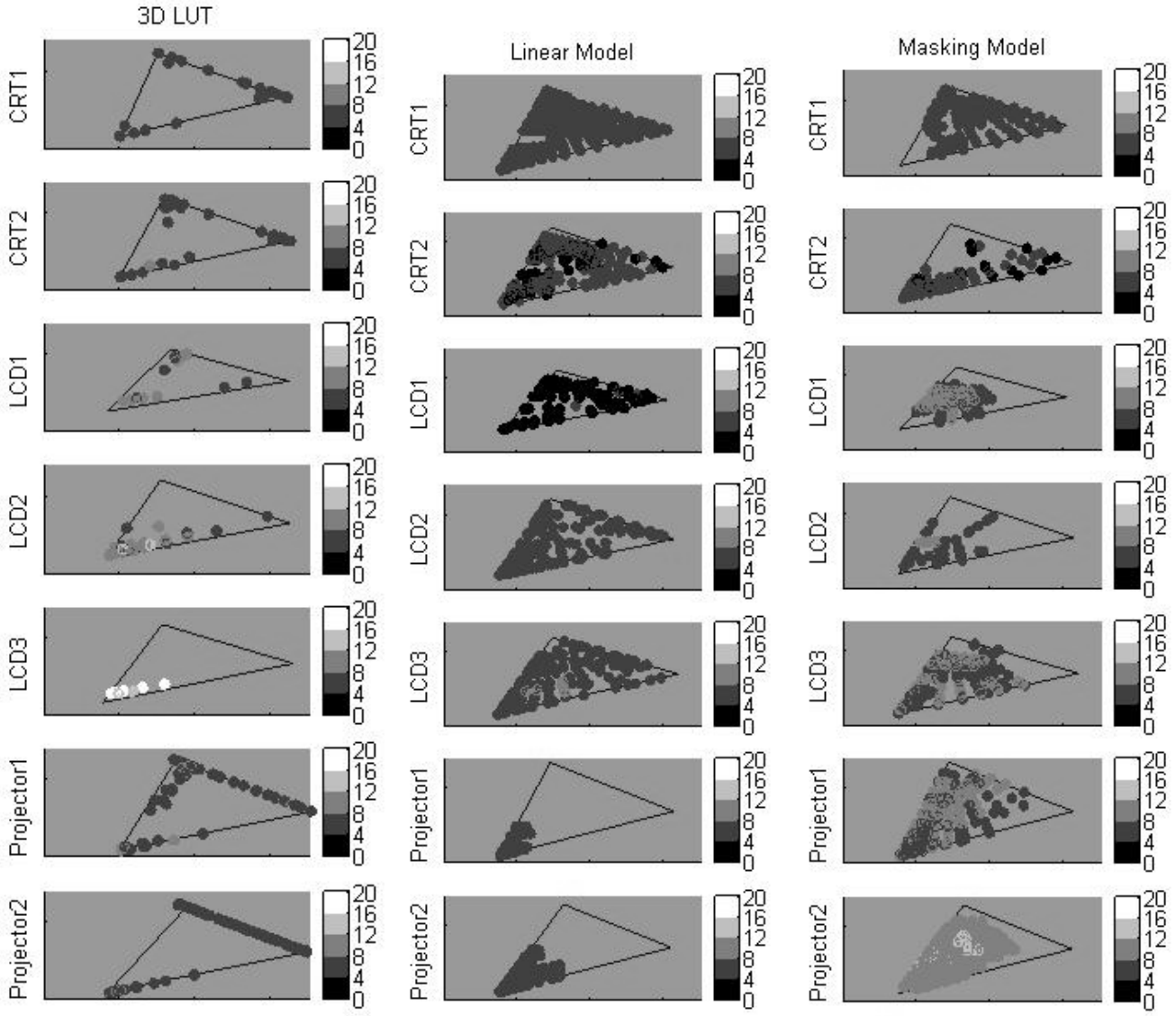

Figure XIX: *Comparison of Outliers for the Backward model. Vertical axis and horizontal axes represent Y./(X+Y+Z) and X./(X+Y+Z) respectively. The • E error is plotted according to the legend of gray scales. The circular points represent outliers with • E greater than 1.5 times the average error. The majority of the high outlier errors for the LUT model occur near the gamut boundaries. . The outliers for linear model are quite negligible compared to the other two models.*

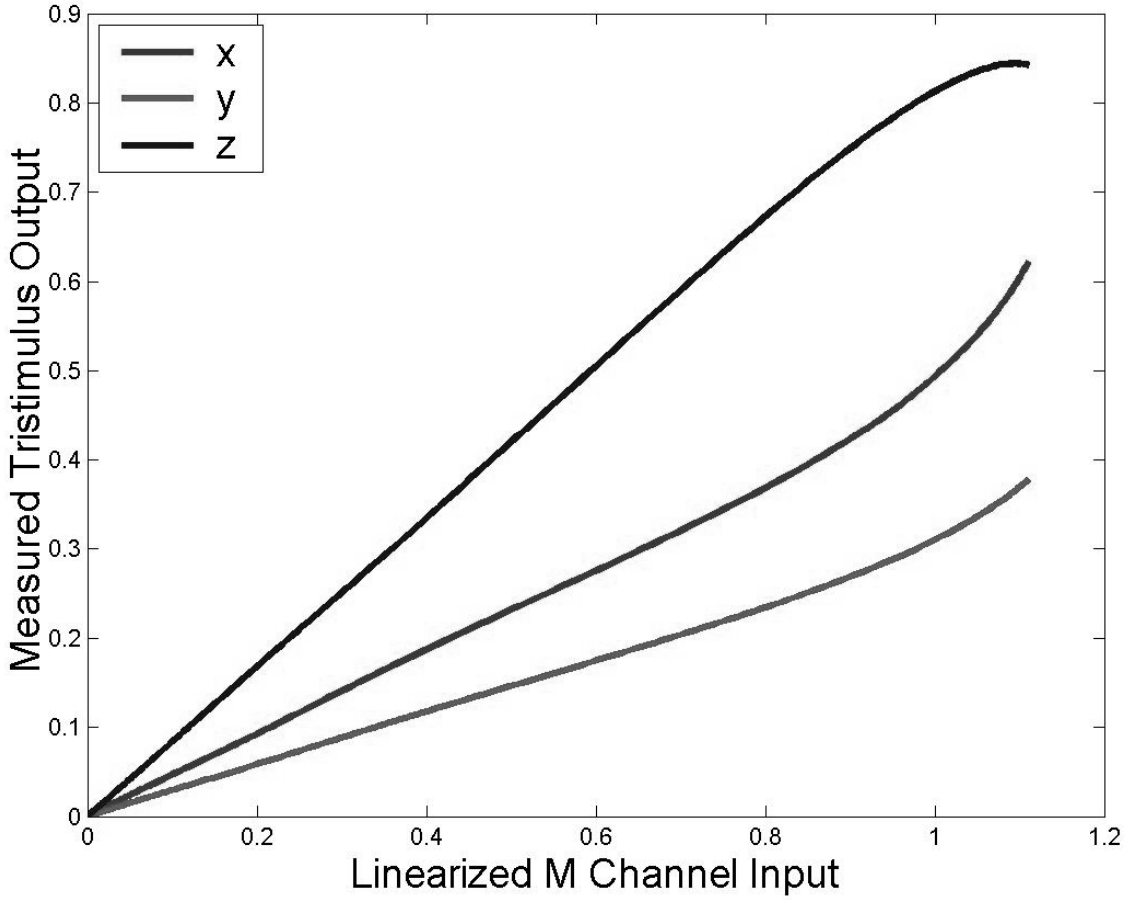

Figure XX: Linearization failure for the black channel on PR1

Tables

Table I: Device Summary

Name	Description	Interaction Mean	Interaction Max
CRT1	Samsung Syncmaster 900NF	2.1%	9.4%
CRT2	NEC Accusync 95F	1.5%	4.9%
LCD1	IBM 9495	0.2%	0.4%
LCD2	NEC 1700V	2.2%	4.1%
LCD3	Samsung 171N	1.2%	2.7%
PR1	Proxima LCD Desktop Projector 9250	0.2%	0.5%
PR2	Proxima LCD Ultralight LX	0.4%	0.7%

Table II: Forward mapping error: ΔE Mean (μ), standard deviation (σ), and maximum.

	LUT			Lin			Lin+			Mask		
	μ	σ	max	μ	σ	max	μ	σ	max	μ	σ	max
CRT1	0.8	0.3	2.4	2.4	1.2	5.4	2.2	1.3	5.2	2.6	1.3	7.1
CRT2	0.5	0.3	2.3	1.7	0.9	4.5	2.7	1.1	6.1	1.5	0.9	4.7
LCD1	0.8	0.8	3.5	0.9	0.5	3.0	0.9	0.6	2.9	3.5	2.8	11.2
LCD2	0.9	0.7	4.2	3.1	1.1	6.5	3.2	1.6	9.7	3.3	1.6	10.4
LCD3	1.0	0.6	4.0	3.7	1.7	8.9	3.7	1.8	9.0	4.2	2.3	11.6
PR1	1.4	1.0	4.5	1.7	1.2	6.5	1.9	1.3	7.2	5.6	2.2	12.3
PR2	0.3	0.2	1.0	2.1	1.1	6.5	2.6	1.3	7.2	7.3	3.3	15.0
Average	0.8			2.2	1.1	5.9	2.5	1.3	6.8	4.0	2.1	10.3

Table III: Backward Error ΔE Mean (μ), standard deviation (σ), and maximum.

	LUT			Lin			Lin+			Mask		
	μ	σ	max	μ	σ	max	μ	σ	max	μ	σ	max
CRT1	1.5	0.9	6.1	2.4	1.2	5.4	2.2	1.3	5.2	2.6	1.3	7.1
CRT2	1.6	1.1	7.6	1.7	0.9	4.5	2.7	1.1	6.1	1.5	0.9	4.7
LCD1	1.8	1.6	11.6	0.9	0.5	3.0	0.9	0.6	2.9	3.5	2.8	11.2
LCD2	2.4	2.2	13.2	3.1	1.1	6.5	3.2	1.6	9.7	3.3	1.6	10.4
LCD3	2.7	3.2	27.6	3.7	1.7	8.9	3.7	1.8	9.0	4.2	2.3	11.6
PR1	2.8	1.8	10.7	1.7	1.2	6.5	1.9	1.3	7.2	5.6	2.2	12.3
PR2	1.9	1.5	8.9	2.1	1.1	6.5	2.6	1.3	7.2	7.3	3.3	15.0
Average	2.1			2.2	1.1	5.9	2.5	1.3	6.8	4.0	2.1	10.3

Table IV: Experimental cpu time and storage space relative to the time and space used by the Linear Model

	Time	Space
Linear	1.0	1.0
Masking	1.2	2.3
3D LUT	17.0	333.4

Table V: Percent Increase in Forward ΔE Error Due to Monotonicity Correction using linear model

	Uncorrected	Corrected	% Increase
CRT1	**2.4**	**2.4**	**0.0%**
CRT2	**1.7**	**1.7**	**0.0%**
LCD1	**0.9**	**0.9**	**-0.7%**
LCD2	**3.1**	**3.1**	**0.0%**
LCD3	**3.5**	**3.7**	**4.7%**
PR1	**1.5**	**1.7**	**12.4%**
PR2	**2.1**	**2.1**	**-0.8%**
Average	**2.2**	**2.2**	**2.3%**

References

1. Amidror I. Scattered data interpolation methods for electronic imaging systems: a survey. *J Electronic Imaging* 2002; 11.2:157-176.
2. Raja Balasubramanian, Reducing the Cost of Lookup Table Based Color Transformations, *Proc. IS&T/SID Seventh Color Imaging Conference* 1999. Vol 44, no.4; p. 321-327.
3. Burns, R. S., Methods for Characterizing CRT displays, *Displays*, Volume 16, Issue 4, 1996, 173-182
4. IEC 61966-4: Multimedia system and equipment: Color measurement and management. Part 4: Equipment Using Liquid Crystal Display Panels, International Engineering Consortium, http://www.map.tu.chiba-u.ac.jp/IEC/100/TA2/parts/index.html, 2000
5. Fairchild MD, Wyble DR. Colorimetric Characterization of the Apple Studio Display (Flat Panel LCD). *Munsell Color Science Laboratory Technical Report*, 1998, http://www.cis.rit.edu/mcsl/research/PDFs/LCD.pdf
6. Finlayson G.D., Drew M.S., White-Point Preserving Color Correction, *Proc. IS&T/SID 5th Color Imaging Conference: Color, Science, Systems and Applications*, pp.258-261, Nov. 1997
7. Gibson JE, Fairchild MD. Colorimetric Characterization of Three Computer Displays (LCD and CRT), *Munsell Color Science Laboratory Technical Repor*t, 2000, , http://www.cis.rit.edu/mcsl/research/PDFs/GibsonFairchild.pdf
8. Kwak Y, MacDonald LW. Accurate Prediction of Colors on Liquid Crystal Displays. *Proc. IS&T/SID 9th Color Imaging Conference* 2001; 355-359.
9. Tamura N, Tsumura N, Miyake Y. Masking Model for accurate colorimetric characterization of LCD. *Proc. IS&T/SID 10th Color Imaging Conference* 2002; 312-316.
10. Yasuhiro Yoshida and Yoichi Yamamoto , Color Calibration of LCDs. *Proc. IS&T/SID 10th Color Imaging Conference* 2002; 305-311.
11. Gabriel Marcu, Gray Tracking Correction for TFT-LCDs, *Proc. IS&T/SID Tenth color imaging conference*, 2002; 272-276